Stabilisation of Electric Arc Furnace Dust by Cementitious Materials: Influence of pH

G. Laforest[1,2], J. Duchesne[2]
[1]*COREM, Québec, Canada;* [2]*Université Laval, Québec, Canada*

Abstract

This study investigates the stabilisation of electric arc furnace dusts (EAFD), a multi-elements toxic waste, influenced by pH. The challenge is to understand the solubility of metal-bearing phases according to pH.

Solubilization tests at different pHs (3-5-7-10-13) were run on EAFD mixed with 0, 25, and 75% of cementitious materials. The concentration of metals (Cr-Ni-Pb-Zn) were analysed in leachates.

The analyses revealed that Cr was fixed at pH <5, Pb between pH 5 and 10, and Ni and Zn at pH >10. The metal-bearing phases were determined by X-Ray Diffraction (XRD), Scanning Electron Microscopy and geochemical modeling. The Zn and Ni-bearing phases were $(Ni,Zn)Fe_2O_4$, (Zn,Mo)O and $Ni(OH)_2$. No Pb-bearing phase was observed but $Pb(OH)_2$ was predicted by the model. Hydrocalumite, identified by XRD, and Cr(VI)-ettringite and $CaCrO_4$, predicted by the model, were the probable Cr-bearing phases.

Cementitious materials have been effective for the reduction of metal concentrations in the leachates.

1. Introduction

EAFD is a listed hazardous waste under Resource Conservation and Recovery Act (RCRA) in United States and under the Transportation of Dangerous Goods Regulations (TDGR) in Canada. High levels of several contaminants cause it to fail the Ontario Regulation 347 leachate extraction procedure [1]. Thus, the untreated disposal of these industrial solid toxic wastes is an environmental risk. Chromium (VI) is particularly problematic because it must initially be reduced before fixed in an insoluble phase.

To mitigate chromium contamination from EAFD, this study investigates the stabilisation and solidification process (S/S). This process aims to limit

Corresponding author:
Guylaine Laforest
COREM, 1180, rue de la Minéralogie, Québec (Québec) Canada G1N 1X7
guylaine.laforest.1@ulaval.ca

the solubility of metals. Precipitate secondary phases (metal-bearing phases) allowed decreasing the solubility of metals. The identification of secondary phases is often not possible because the quantities are too low to be detected by ordinary means (X-Ray Diffraction or Scanning Electron Microscope analyses). The geochemical modeling is a tool to help the determination of possible metals-bearing phases.

The immobilisation of Cr in cement matrices can occurs in many ways. Cr (III) can precipitate as $Cr(OH)_3$ and/or be substituted in cement hydrates such ettringite ($3CaO•Al_2O_3•3CaSO_4•32H_2O$) and calcium monosulfoaluminate hydrate ($3CaO•Al_2O_3•CaSO_4•12H_2O$) or in calcium silicate hydrate (C-S-H) [2]. Cr (VI), which primarily occurs as CrO_4^{2-} in alkaline solutions [3,4], can substitute for the SO_4^{2-} in ettringite [5] and in monosulfate [2,4]. The substitution of Cr (III) for Al (III) in calcium aluminate hydrates formed by the hydration of GGBFS is also possible [6]. GGBFS has a reducing potential that would create an environment where the Eh values (-200 to -400 mV) will be more reducing than in a system composed mainly of Portland cement (100 to 200 mV) [6,7].

However, several studies have shown that there is no solubility control on chromium in cement-based S/S technology [8,9,10,11]. Thus Cr, in particular Cr (VI), remained free in the leachate. To solve this problem with conventional cement-based S/S process, it is possible to use GGBFS which develops, according to many authors, phases able to exert a solubility control on chromium [3,6,8,10,11,12,13].

A recent study on chromium binding isotherms by Laforest and Duchesne [14] has shown that GGBFS and ordinary Portland cement (OPC) were both effective to fix Cr (VI). The OPC exerted a better solubility control for Cr concentrations in solution higher than 1 000 mg/L, while the GGBFS was more efficient at low Cr concentrations. For samples in solution with initial Cr (VI) concentrations between 1 000 to 50 000 mg/L, the Cr-bearing phases identified were $CaCrO_4$, $CaCrO_4•2H_2O$, calcium silicate hydrates (C-S-H) and calcium aluminate hydrates (hydrocalumite (C_4AH_{13})).

2. Purposes

The purpose of this study is to investigate the potential of GGBFS and OPC in fixing Cr ions and selected heavy metals (Ni, Pb and Zn) leached from the EAFD. The challenge is to understand the solubility of metal-

bearing phases according to pH. Iron was not the subject of a particular follow-up despite its important content in the EAFD (28%). Cr, Ni, Pb and Zn were studied due to their important quantities in the EAFD and also because these metals appear on the list of regulated toxic metals.

3. Materials

The GGBFS was provided by Algoma Steel (Sault Ste-Marie, Canada). This slag, cooled quickly, is largely in a glassy form with a small proportion of merwinite and of solid-solution of the melilite family. An ordinary Type I cement was used in this study. The chemical compositions of the solid materials are given in Table 1.

The EAFD was supplied by Atlas Stainless Steels (Sorel, Canada) and was obtained in the summer of 2000. Table 1 presents the chemical composition of the major oxides of the EAFD tested in this work. The EAFD has a bimodal size distribution. Particle sizes ranged from less than 2.8 μm to greater than 176 μm. The majority (94%) of the particles were smaller than 5.5 μm in diameter. Magnetite was the main phase present in the EAFD, along with chromite. Most grains were identified as franklinite-magnetite-jacobsite solid solutions.

Table 1. Chemical composition of materials

Oxides (% mass)	CaO	SiO_2	MgO	Al_2O_3	MnO	Fe_2O_3	K_2O	TiO_2	Na_2O	LOI*	Total
GGBFS	37.31	36.77	13.91	7.77	1.02	0.85	0.43	0.36	0.31	-1.49	97.23
OPC	62.49	19.75	2.62	4.41	0.05	2.92	0.89	0.17	0.28	1.90	95.48
EAFD	6.59	5.76	4.25	0.74	5.88	39.56	0.48	0.16	1.01	3.67	68.10

*LOI= loss on ignition

4. Methods

4.1. Toxicity Characteristic Leaching Procedure (TCLP)

The Toxicity Characteristic Leaching Procedure (TCLP) (EPA (Method 1311)) [15] is a standard leaching test to determine the degree of toxicity of waste. TCLP was run on the EAFD sample.

4.2. Solubilization tests at different pHs

Solubilization tests at different pHs (3-5-7-10-13) were run on EAFD mixed with 0, 25, and 75% of cementitious materials The formulations used are presented in Table 2.

The samples were placed in 60 ml high density polyethylene containers and mounted horizontally on a Plexiglass carousel immersed in a temperature bath at 25°C ± 0.5°C. The carousel was rotated between 10 and 20 rpm for 72 hours without interruption. The 3 days required to reach equilibrium were retained in accordance with Perkins and Palmer [14] whose studied the solubility of chromate hydrocalumite. The authors adopted a reaction time of 14 days and mention that this time is well after the 2 days necessary to reach the steady-state concentrations of species being analyzed. To establish the pH values where metals were precipitated in an insoluble phase, leachants were made up solutions with NaOH and HCl at pH 3, 5, 7, 10 and 13. The pH was adjusted twice a day by an HCl or NaOH addition to maintain the initial pH value of the immersion solution.

Table 2. Mixture characteristics of monolithic specimens

Formulation	% GGBFS	%OPC	%EAFD
EAFD	0	0	100
25 GGBFS :75 EAFD	25	0	75
75 GGBFS :25 EAFD	75	0	25
25 OPC :75 EAFD	0	25	75
75 OPC :25 EAFD	0	75	25

4.3. Chemical analysis method

Solution samples were filtered through 0.22 µm membrane filters and acidified with HCl for cation analyses (Cr, Ni, Pb and Zn) on a Perkin Elmer Aanalyst 100 Atomic Absorption Spectrophotometer (AAS). The AAS detection limits for Cr, Ni, Pb and Zn are 0.078, 0.14, 0.19 and 0.018 mg/L, respectively. All solutions were kept at 4°C until analysis.

4.4. Mineralogical characterisation

The mineralogy characterisation was made by X-Ray Diffraction (XRD) and Scanning electron microscope (SEM) analyses. Specimens were analyzed by a Siemens D5000 X-Ray diffractometer using Cu Kα radiation generated at 20 mA and 40 kV. The specimen was step-scanned as

random powder mounts from 2-62.8° 2θ at 0.02° 2θ steps integrated at 1.2 s $step^{-1}$. XRD analysis can detect crystalline phases presented on the order of about 5% by mass or more. Specimens were observed also under a JEOL 840A SEM equipped with an energy dispersive X-ray (EDX) analysis system.

5. Results and discussion

5.1. TCLP results

The TCLP results and the heavy metals content of EAFD are presented in Table 3. Total Cr (9.7 mg/L) and the Cr (VI) (6.1 mg/L) concentrations are over the value of Toxicity Characteristic Regulatory Level (Table 3) while the Pb concentration is under the regulatory level. Ni and Zn concentrations are not regulated by the TCLP but Zn reaches high concentration (93.9 mg/L). We did not run TCLP on stabilized mixtures with OPC and GGBFS because we judged that this test is not appropriate for S/S formulations. Indeed, the final pH of the TCLP test (4.93) is very low relative to the pH of S/S products (approximately 13).

Table 3. Heavy metals content and TCLP results for EAFD

Heavy metals	[Cr_{Total}]	[Cr (VI)]	[Ni]	[Pb]	[Zn]
EAFD (%mass)	10.9	-	4.1	1.4	5.2
TCLP results (mg/L)	9.7	6.1	2.3	0.4	93.9
TCRL (mg/L)	5.0	-	-	5.0	-

TCLP: Toxicity Characteristic Leaching Procedure
TCRL: Toxicity Characteristic Regulatory Level [15]

5.2. Solubilization test results

The Fig. 1 shows the solubilization test results after 3 days of reaction at fixed pHs. The graphs on the right side of the Fig.1 are the modeled results obtained by MINTEQA2 and are discussed in the next section (5.2.1). Chromium was not found in leachate at low pH, < 5. Starting from a pH value of 5, Cr was increasingly free in solution with higher pHs. The maximum Cr concentration in solution was observed for the EAFD sample at pH 13. At high pHs, both binders (with a similar percentage) offered comparable performance in fixing Cr ions.

Lead was not found in leachate for pHs between 5 and 10, for all mixtures. At low pHs, GGBFS (with a large percentage; 75 GGBFS: 25 EAFD) was more effective than OPC in reducing Pb concentrations. At pHs higher than 10, the OPC had a slightly better performance than GGBFS in

reducing Pb concentrations. The Pb solubility is lower between pH values of 5 and 10.

Zn concentrations decreased gradually from pH 3 to 7. For pH 7 or higher, Zn concentrations were under the detection limit. The GGBFS and OPC decreased the amount of Zn in solution in a similar way.

Ni showed exactly the same behaviour as Zn, with a decrease in concentration from pH 3 to 7. As for Zn, Ni was under the detection limits for pH equal or higher to 7.

According to these results and knowing that the pH existing in the pore solutions of cement-based materials (are approximately 13), the 75 OPC: 25 EAFD formulation was the better mixture to stabilize EAFD. However, the concentrations of Cr are high (9 mg/L). The 75 OPC: 25 EAFD sample will also presents a good performance if the pH decreases. The XRD analysis revealed that the 75 OPC: 25 EAFD sample is composed of calcite, portlandite, nickel zinc iron oxides ($(Ni,Zn)Fe_2O_4$), magnesioferrite ($MgFe^{2+}{}_3O_4$) and hydrocalumite which appears like hollow rods by SEM observations (Fig. 2A). No Cr and/or Pb-bearing phase was found. However, the hydrocalumite is a possible Cr-bearing phase as previously noted in section 1. GGBFS sample (75 GGBFS: 25 EAFD) was less efficient at pH 13 compared to OPC in fixing Cr ions. The XRD analysis of GGBFS sample showed that it was mainly amorphous, probably due to the presence of not hydrated phase according to the short reaction time (3 days) and the slow hydration of GGBFS. It is composed of calcite which appeared mainly as the classic scalenohedron form (Fig. 2B), nickel zinc iron oxide and magnesioferrite. No portlandite and hydrocalumite were observed on the GGBFS sample.

5.2.1. Geochemical modeling

Geochemical modeling was run to help the identification of the possible metal-bearing phases eludes detection by XRD and SEM techniques. The relative amount of elements in solution and relative amount of predicted precipitated phases were evaluate with the geochemical speciation model Visual MINTEQ version 2.30 (a program based on MINTEQA2 version 4.0) [16]. It is important to note that certain simplifications were made to allow the prediction of the behaviour of heavy metals in contact or not with binders (GGBFS and/or OPC). In the model, the composition of all solid materials (GGBFS, OPC and EAFD) was regarded as having completely been solubilized. This was not the case in our experiment where some EAFD particles were still more or less intact after the leaching experiment. So, in the model the EAFD original phases identified by XRD or SEM and present in the database (spinel, periclase, magnetite, hematite and chromatite) were included like phases which will not dissolve completely during the equilibration. Quartz, chalcedony and cristobalite were

excluded from the model. Also, some phases normally present in the hydrated binders are not included in the geochemical speciation model. For example, C-S-H is not included in the database of Visual MINTEQ version 2.30. It is important to note that the goal of the modeling was not to reproduce exactly the concentrations of leachate but to reproduce the behaviour of heavy metals according to the different pH conditions and especially to identify the possible metal-bearing phases. In the model, only the principal elements (H_4SiO_4, Ca(II), Al(III), Fe(II), CrO_4^{2-}, Mn(II), Mg(II), Ni(II), Pb(II) and Zn(II)) of the solid materials were considered.

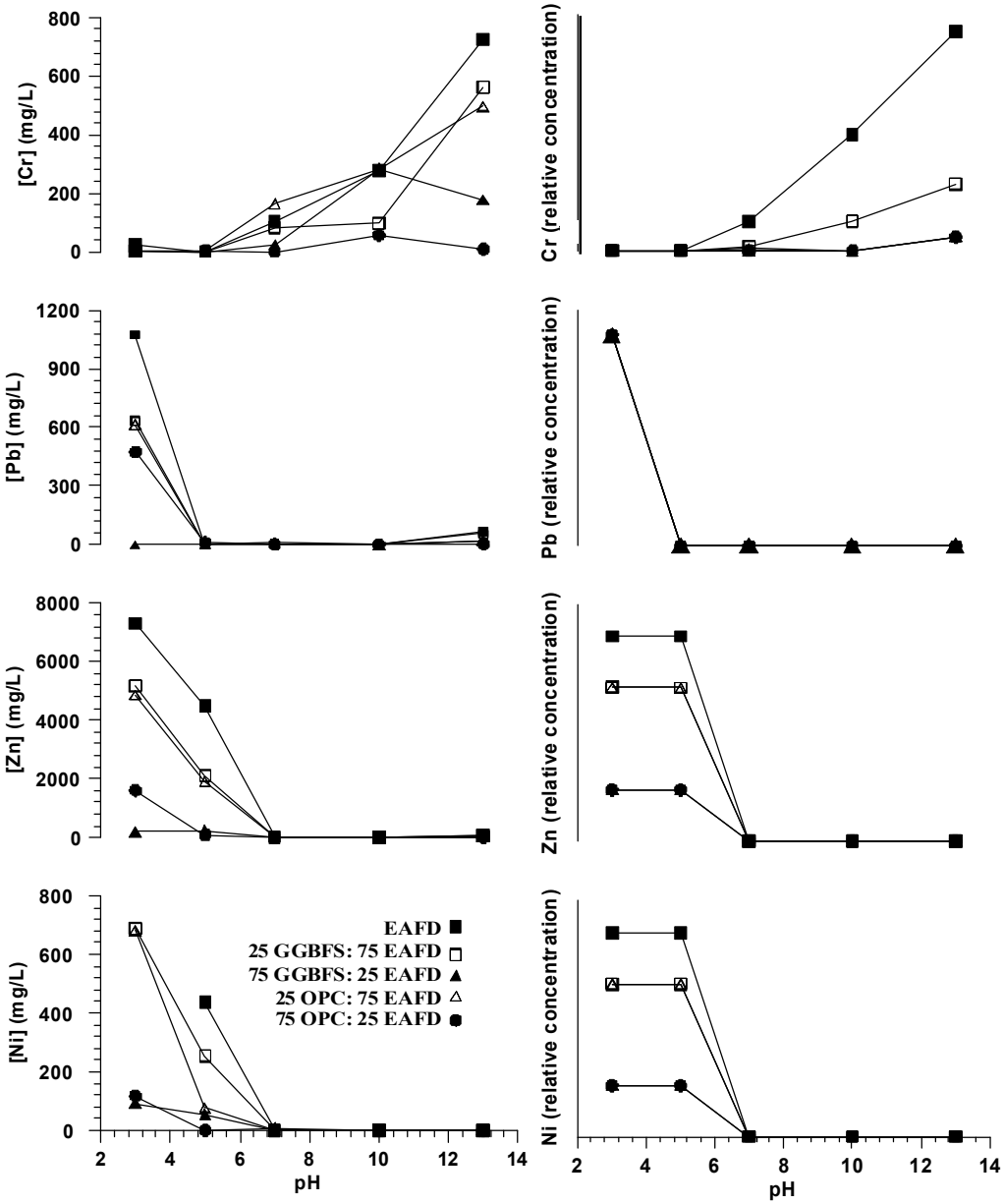

Fig. 1. Experimental and modeled results of leached metals as function of pH.

The modeled results of leached metal as a function of pH are presented in Fig.1. The general tendency of the curves compared well with the experimental results. The model was significant to estimate the behaviour of the heavy metals from EAFD according to the pH conditions and some general conclusions can be drawn. The solubility decreased starting from a of pH 5 for Pb and from a pH of 7 for Zn and Ni. Chromium presents an inverse behaviour with concentrations increasing from pH 5 to more basic environment. One modeled result differs from experimental one; modeled Pb concentrations were very low (insoluble) at pH of 13 compared to the experimental results. The Pb-bearing phase proposed by the model was $Pb(OH)_2$. In spite of the high solubility of $Pb(OH)_2$ at alkaline pH (133 mg/L) [17], this lead hydroxide is a stable phase at alkaline pH when the concentration of lead ions is high [18]. In the real experiment, the partial solubilization of Pb's EAFD and the probable incorporation of some Pb ions in C-S-H imply that the Pb ions concentration was probably not enough to precipitate $Pb(OH)_2$. This implies that some real phases incorporating Pb and having a solubility which increases at pH 13 were not included in the model. This phase may be a lead carbonate where the Ca^{2+} can be release for the subsequent precipitation of portlandite and/or Cr(VI)-ettringite for example. Lead carbonate ($PbCO_3$) and basic lead carbonate ($Pb_3(CO_3)_2(OH)_2$), two phases not included in the model, are much less soluble than lead hydroxide [19]. The solubility of $PbCO_3$ and $Pb_3(CO_3)_2(OH)_2$ in alkaline pH were 0.85 and 1.3 mg/L respectively [17]. These existing phases in the EAFD would attenuate the solubilization of Pb.

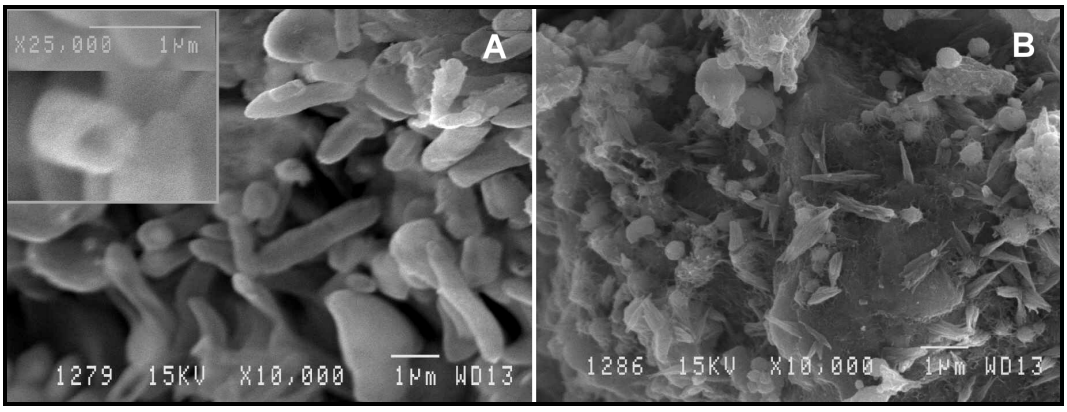

Fig. 2. SEM pictures in secondary electrons of 75 OPC: 25 EAFD (A) and 75 GGBFS: 25 EAFD (B) samples in basic solution (pH13) after 3 days.

The modeled results confirm that the best results, according to the reduction in the concentration of contaminants, were obtained with the 75

OPC: 25 EAFD sample for all values of pH. At pH 13, the pH of the cement-based pore solution, the concentrations of Ni, Pb and Zn were null. The concentration of Cr was under 3.5 mg/L. The Cr(VI)-ettringite is precipitated for all sample at pH 13 (Fig. 3). The model uses 99.9% of Ca^{2+} and 80.5% of CrO_4^{2-} for the formation of Cr(VI)-ettringite. The lack of Al is filled, by the model, by the solubilization of the spinels. Thus, in this case, the formation of Cr(VI)-ettringite is function of the availability of Ca^{2+} for all samples.

A difference between modeled and experimental values was observed between pH 3 and 5 where concentrations of Zn and Ni were stable in the modeled values while they were decreasing in the experimental ones. This tendency was also showed in the samples without binder for Zn and Ni (Fig. 1). This is probably due to the formation of Ni or Zn carbonates. This confirms that some Ni and Zn-bearing phases are not included in the model. The mineral saturation index calculations of the new precipitated phases show that a nickel hydroxide ($Ni(OH)_2$) was probable Ni-bearing phase while zincite ((Zn,Mo)O was probable Zn-bearing phase.

Lead presents different behaviours at high pH between modeled and experimental data. For all mixtures, the calculated curves showed Pb concentrations decrease starting from pH 5. According to the experimental results, Pb concentrations were almost nulls between the pH 5 and 10, and then increased at pH 13. This concentration increasing was not found on the modeled curve. This supposes that certain phases are missing in the model and thus not included in the modeled results. The mineral saturation index calculations of the new precipitated phases show that $PbCrO_4$ and $Pb(OH)_2$ were probable Pb-bearing phases.

The mineral saturation index calculations of the new precipitated phases show that $PbCrO_4$, $MgCrO_4$ and Cr(VI)-ettringite ($Ca_6[Al(OH)_6]_2(CrO_4)_3.26H_2O$) were probable Cr-bearing phases. The relative amounts of possible Cr -bearing phases are presented in Fig. 3 according to pH values. Modeling shows that the solubility of $CaCrO_4$ is slightly under saturated conditions between the pH of 5 to 13, particularly between pH 7 and 10. This phase, slightly under saturated conditions according to the model, was identified by XRD and SEM by Laforest and Duchesne [14]. The pHs where the Cr(VI)-ettringite is oversaturated varied with the sample and the precipitation can start from pH value of approximately 9 to 12. These two phases (Cr(VI)-ettringite and $CaCrO_4$) along with C-S-H are the most probable Cr-bearing phase in cement-based material. The model confirms the presence of Cr(VI)-ettringite. The hydrocalumite observed by XRD is not included in the model. The

chromate hydrocalumite ($3CaO.Al_2O_3.CaCrO_4.nH_2O$) is a more stable phase than the Cr(VI)-ettringite and it is a probable Cr-bearing phase.

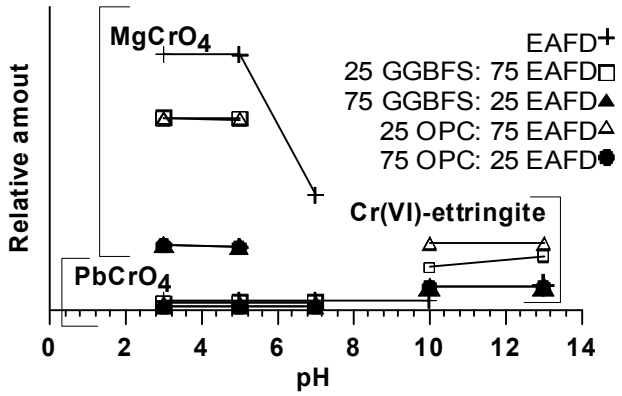

Fig. 3. The modeled Cr-bearing phases precipitated according to the pH.

6. Conclusions

The analyses revealed that Cr was fixed at pH <5, Pb between pH 5 and 10, and Ni and Zn at pH >10. The metal-bearing phases were determined by X-Ray Diffraction (XRD), Scanning Electron Microscopy and geochemical modeling. The Zn and Ni-bearing phases were $(Ni,Zn)Fe_2O_4$, (Zn,Mo)O and $Ni(OH)_2$. No Pb-bearing phase was observed but $Pb(OH)_2$ was predicted by the model. Hydrocalumite, identified by XRD, and Cr(VI)-ettringite and $CaCrO_4$, predicted by the model, were the probable Cr-bearing phases.

Acknowlegments

This study has been supported by the National Science and Engineering Research Council of Canada (NSERC) and by the Fonds de recherche sur la nature et les technologies of the Province of Québec (FQRNT). The authors would like to thank also Atlas Stainless Steels in Sorel, Canada.

References

[1] R.J. Caldwell, C. Shi, J. A. Stegemann, Solidification formulation development for a speciality steel slectric arc furnace dust. in: Cases, J. M., Thomas F. (Eds.), International Congress on Waste Solidification-Stabilisation Processes. Société Alpine de Publications, Grenoble, France, 1995, pp.148-158.

[2] S. Takahashi, M. Daimon, E. Sakai, Sorption of CrO_4^{2-} for cement hydrates and the leaching from cement hydrates after sorption. in: Grieve, G., Owens, G. (Eds.), 11th International Congress on the Chemistry of Cement (ICCC) "Cement's Contribution to the Development in the 21st Century", The Cement and Concrete Institue of South Africa, Durban, South Africa, 2003, pp.2166-2173.

[3] D.E. Macphee, F. P. Glasser. Immobilization science of cement systems. MRS Bulletin 18 (1993) 66-71.

[4] R.B. Perkins, C. D. Palmer, Solubility of chromate hydrocalumite ($3CaO{\cdot}Al_2O_3{\cdot}CaCrO_4.nH_2O$) 5-75°C. Cem Concr Res 31 (2001) 983-992.

[5] R.B. Perkins, C. D. Palmer, Solubility of $Ca_6[Al(OH)_6]_2(CrO_4)_3{\cdot}26H_2O$, the chromate analog of ettringite; 5-75°C. Appl. Geochem. 15 (2000) 1203-1218.

[6] A. Kindness, A. Macias, F. P. Glasser, Immobilization of chromium in cement matrices. Waste Manage 14 (1994) 3-11.

[7] F.P. Glasser, F. P., Fundamental aspects of cement solidification and stabilisation. J Hazard. Mater. 52 (1997) 151-170.

[8] A. Macias, S. Goni, J. Madrid, J. M. Diez, E. del Castillo, Potential of blast furnace slags to immobilize toxic wastes. in: Malhotra, V. M. (Ed.), Fly ash, Silica Fume, Slag and Natural Pozzolans in Conrete. Canada Centre for Mineral and Energy Technology (CANMET), American Concrete Institute, Bangkok, Thailand. 1998, pp. 893-909.

[9] J.N. Diet, P. Moszkowicz, A. Navarro., Solidification de boues d'hydroxydes métalliques par des ciments Portland: comportement du ciment en présence de boues d'hydroxyde de chrome. in: Cases, J. M., Thomas F. (Eds.), =International Congress on Waste Solidification-Stabilisation Processes. Société Alpine de Publications, Grenoble, France, 1995, pp. 207-212.

[10] M.L. Allan, L. E. Kukacka, Blast furnace slag-modified grouts for *in situ* stabilization of chromium-contaminated soil. Waste Manage 15 (1995) 193-202.

[11] J. Duchesne, J., Réduction des concentrations en Cr et en Mo dans des lixiviats générés par des poussières de four de cimenterie. in : Méhu, J., Keck G., Navarro A. (Eds.), Stabilisation des Déchets & Environnement 99, Lyon-Villeurbanne, France, 1999, pp. 21-25.

[12] S.K. Srivastava, V. K. Gupta, D. Mohan, Removal of lead and chromium by activated slag - A blast-furnace waste. J. Environ. Eng. 123, (1997) 461-468.

[13] J. Duchesne, G. Laforest, Evaluation of the degree of Cr ions immobilization by different binders. Cem Concr Res 34 (2004) 1173 - 1177.

[14] G. Laforest,J. Duchesne, Immobilization of chromium (VI) evaluated by binding isotherms for ground granulated blast furnace slag and ordinary Portland cement. Cem Concr Res 35 (2005) 2322-2332.

[15] EPA (U.S. Environmental Protection Agency),. Test methods for evaluating solid waste, physical/chemical methods (SW 846), National Technical Information Service, 1997.

[16] J.P. Gustafsson, J. P., Visual MINTEQ, version 2.30. KTH, Dept. of Land and Water Resources Engineering, Stockholm, Sweden, 2004.

[17] J.R. Conner, J. R., Chemical fixation and solidification of hazardous wastes. Van Nostrand Reinhold, New York, 1990.

[18] M. Pourbaix, M., Atlas of electrochemical equilibria in aqueous solutions, Second English edition, Houston, Texas, USA. 1974.

[19] J.R. Conner, Guide to improving the effectiveness of cement-based stabilization/solidification. Engineering bulletin EB211. Portland Cement Association, Skokie, Illinois, 1997.